Advanced non-linear control algorithms applied to design highly maneuverable Autonomous Underwater Vehicles (AUVs)

Vladimir Djapic, Jay A. Farrell, Paul Miller, and Rich Arrieta

Abstract— **An increasing variety of sensors are becoming available for use onboard autonomous vehicles. Given these enhanced sensing capabilities, scientific and military personnel are interested in exploiting autonomous vehicles for increasingly complex missions. Most of these missions require the vehicle to function in complex, cluttered environments and react to changing environmental parameters. The present state-of-art vehicles are not maneuverable enough to successfully accomplish most of these tasks. In this research, a nonlinear controller was derived, designed, implemented in simulation and onboard a AUV, and in-water tested in order to enhance vehicle maneuverability. The structure of a controller is hierarchical such that an "inner loop" non-linear controller (outputs the appropriate thrust values) is the same for all mission scenarios while a library of "outer-loop" non-linear controllers are available to implement specific maneuvering scenarios. On top of the outer-loop is the mission planner which selects which outer-loop controller will be used. The algorithms are generic and in no way vehicle specific and can therefore be implemented on various AUVs.**

I. INTRODUCTION

Autonomous Underwater Vehicles (AUVs) are being considered for chemical plume tracing [3], [5], [6], [7], mine-countermeasures (MCM) [9], and ship hull search [2]. AUVs equipped with high-level control software have a variety of potential applications for Anti-Terrorism/Force Protection (ATFP) objectives. In this paper we present the design and the implementation of the advanced control algorithms onboard the SPAWAR Systems Center's ship hull inspection platform. In addition, we show the latest accomplishments at the Autonomous Underwater Vehicle Festival (AUVFest), June 6-15 2007, held in Panama City. During this effort we leveraged the existing vehicle sensors and improved their use by introducing novel control and navigation techniques. Vehicle dynamics, its sensors, and the environmental factors, such as currents, are modeled in a comprehensive vehicle simulation. Our software simulates sensor noise and performance characteristics, range measurements, acoustic angle of incidence and line-of-sight requirements, and random drop outs. Simulation environment can import 3D models of arbitrary solid objects, such as ship hulls, sea floor terrain maps, quay walls, pier pilings, etc. The same vehicle and control software that is executed in simulation is executed onboard of the AUV. This approach significantly reduces costly in-water testing requirements as well as provides mission plan verification. This approach accelerates vehicle navigation, control, and mission development since we can experiment with operational challenges without asset risk. Moreover, the simulator can be used as a great operator training tool through basic operator tele-operation training. AUVs equipped with this type of software can greatly enhance current underwater security capabilities, relieving divers of time-consuming, dangerous tasks, therefore, reducing manpower and mission timeline requirements.

This work was supported by Office of Naval Research (ONR) and Space and Naval Warfare Systems Center San Diego (SSC-SD) through In-house Independent Research (ILIR) Program. The implementation of the algorithms onboard of AUV was supported by PMS EOD and EODTECHDIV.

V. Djapic is with Unmanned Maritime Vehicle (UMV) Lab, SSC-SD, San Diego, CA 92152, USA and with the Department of Electrical Engineering, University of California, Riverside (UCR), CA 92521, USA djapic@spawar.navy.mil

J.A. Farrell is with the Department of Electrical Engineering, UCR, Riverside, CA 92521, USA farrell@ee.ucr.edu

P. Miller and R. Arrieta are with Unmanned Maritime Vehicle (UMV) Lab, SSC-SD pamiller@spawar.navy.mil, rich.arrieta@navy.mil

A. Inner Loop Controller Implementation

In this subsection we describe the development of the inner loop controller which computes the desired thrust values to achieve the commanded velocities and angular rates and sends the commands to thrusters which create vehicle movement. The vehicle employed for simulation and in-water testing is a thruster powered vehicle, which is underactuated, since it does not have thrusters, thus, direct control in the lateral direction. Initially, a significant amount of real-time sensor data was collected for analysis by performing various experiments with our test-bed AUV. This data was used to estimate vehicle parameters and characterize the sensors. The vehicle parameters were approximated for all five inner loop control variables. The dynamics equations for horizontal speed (u), vertical speed (w), roll rate (p), pitch rate (q), and yaw rate (r) were derived in terms for non-linear forces acting on the vehicle in each of its five controllable degrees-of-freedom. Using various MATLAB routines, the parameters were approximated for (1) Drag Forces - two parameters per each DOF, (2) Buoyancy Force and Centers of Buoyancy in each 3 directions, (3) Inertia Terms in each direction. These parameters were then used in a Feedback Linearizing controller, whose performance depends on the accuracy of the model. Later on, the expected model uncertainties are compensated for using a novel approach to back-stepping non-linear control technique. The controller compensates well for the hydro forces acting on the vehicle. All inputs to the inner loop (and to each outer loop) are pre-filtered by the filter of the specific structure that we designed. The purpose of this filter is to produce a continuous signal and its derivative such that continuous signal closely tracks command generated (or user specified) desired signal within the bandwidth of the control systems. More on command filtering is elaborated on in the following subsection.

B. Outer Loop Controller Implementation

In this subsection we describe the development of various modes of outer loop controllers which compute the desired velocities and angular rates to achieve a behavior or a specific maneuver. These outer loops include various control modes that generate commands to the inner loop. Each control mode is a set of nonlinear equations that implement a specific maneuver. The vehicle uses the novel translational, attitude, and altitude controller based on the nonlinear control technique called Back-stepping. The novel controller implements the ideas of Back-stepping and, in addition, introduces a new algorithm called Command Filtered (CF) Back-stepping. Several places in this paper refer to filtering of a signal x_c^o to produce a signal x_c and its derivative $\dot{x}_c$. This is referred to as command filtering. The motivation of command filtering is to determine the signals $x_c(t)$ and $\dot{x}_c(t)$ as needed for the next iteration of the backstepping procedure [10], without having to analytically differentiate x_c^o, because the analytic differentiation becomes overly cumbersome for systems of high dimension. The first objective was to control the vehicle's attitude or orientation angles (roll, pitch, and yaw), and to maintain vehicle's depth. This basic outer loop is described in this paper in Section V. We refer to this loop as middle loop controller since it is used by each of the outer loops. Our test-bed AUV is capable of maintaining attitude (roll, pitch, and yaw) using the Back-stepping Attitude Controller (BAC) which outputs appropriate angular rate commands (p_c^o, q_c^o, r_c^o) to the angular rate inner loop. Depth control is achieved using Back-stepping Depth Controller (BDC), which outputs appropriate vertical speed command (w_c^o). Tracking of the desired trajectory is achieved using Back-stepping Trajectory Controller (BTC), which commands appropriate vehicle speed (u_c^o) and yaw (ψ_c^o).

This paper is formatted as follows. Section II defines vehicle dynamics. Section III summarizes the control signals that are implemented. Section IV shows the derivation of the waypoint guidance algorithm. Section V derives the attitude controller. Section VI presents the velocity and angular rate controller. Section VII describes the results from AUVFest. Finally, Section VIII outlines potential new control design.

II. THRUSTER POWERED AUV DYNAMICS

Let the vehicle dynamics be described as [4]

$$\begin{aligned} \dot{p} &= R_b^t v_b && (1)\\ \dot{\Theta} &= \Omega\omega && (2)\\ \dot{v}_b &= M^{-1}(u_1 - F_{nlin}) && (3)\\ \dot{\omega} &= J^{-1}(u_2 - M_{nlin}) && (4) \end{aligned}$$

where $p = [x, y, d]$ is the earth relative position, R_b^t is the rotation from body to earth frame, $v_b = [u, v, w]^\top$ is the velocity in body frame, $\Theta = [\phi, \theta, \psi]$ is the attitude, Ω is a nonlinear (nonsingular except at $\theta = \frac{\pi}{2}$) matrix function of Θ, ω is the inertial rotation rate vector represented in body frame, F_{nlin} represents the body-frame nonlinear forces, M_{nlin} represents the body-frame nonlinear moments, u_1 is the vector of control forces, u_2 is the vector of control moments. The control forces and moments are generated by a set of five thrusters mounted to achieve full angular rate control (i.e., ω), surge control (i.e., u), and heave control (i.e., w). The vector $T = [T_1, \ldots, T_5]^\top$ of five thrusts is related to the the control forces and moments by a known thrust distribution matrix such that $u_1 = L_f T$ and $u_2 = L_m T$ where $L_f \in \Re^{2\times 5}$ and $L_m \in \Re^{3\times 5}$. The AUV is underactauted since the lateral speed v is not directly affected by the thrusters.

The rotation matrix, R_b^t, is defined as

$$R_b^t = \begin{bmatrix} \mathrm{c}\theta\mathrm{c}\psi & \mathrm{c}\psi\mathrm{s}\theta\mathrm{s}\phi - \mathrm{c}\phi\mathrm{s}\psi & \mathrm{c}\phi\mathrm{c}\psi\mathrm{s}\theta + \mathrm{s}\phi\mathrm{s}\psi \\ \mathrm{c}\theta\mathrm{s}\psi & \mathrm{c}\phi\mathrm{c}\psi + \mathrm{s}\theta\mathrm{s}\phi\mathrm{s}\psi & -\mathrm{c}\psi\mathrm{s}\phi + \mathrm{c}\phi\mathrm{s}\theta\mathrm{s}\psi \\ -\mathrm{s}\theta & \mathrm{c}\theta\mathrm{s}\phi & \mathrm{c}\theta\mathrm{c}\phi \end{bmatrix},$$

and the angular rate transformation matrix, Ω, as

$$\Omega = \begin{bmatrix} 1 & \mathrm{s}\phi\mathrm{t}\theta & \mathrm{c}\phi\mathrm{t}\theta \\ 0 & \mathrm{c}\phi & -\mathrm{s}\phi \\ 0 & \mathrm{s}\phi/\mathrm{c}\theta & \mathrm{c}\phi/\mathrm{c}\theta \end{bmatrix},$$

where the symbols c_z, s_z, and t_z represent cos(z), sin(z), and tan(z).

III. CONTROL SIGNALS IMPLEMENTATION

This section summarizes the control law. The stability analysis is rigorously analyzed in [1]. Due to lack of space, the arguments are not repeated herein. The following equations represent the control signals

$$\begin{aligned} u_c^o &= s\frac{\| \ [-F_x - K_{xy}\tilde{x} + \dot{x}_c, -F_y - K_{xy}\tilde{y} + \dot{y}_c] \ \|}{\mathrm{c}\theta} \\ \psi_c^o &= atan2\left[s\left(-F_y - K_{xy}\tilde{y} + \dot{y}_c\right), s\left(-F_x - K_{xy}\tilde{x} + \dot{x}_c\right)\right] \\ w_c^o &= \frac{u\sin(\theta) - \cos(\theta)\sin(\phi)v - K_d\tilde{d} + \dot{d}_c}{\cos(\theta)\cos(\phi)} \\ \omega_c^o &= \Omega^{-1}\left(-K_\Theta\tilde{\Theta} + \dot{\Theta}_c - \Theta_{bs}\right) \\ u_1 &= M(F_{nlin} - K_v\tilde{v}_b + \dot{v}_{bc} - v_{bbs}) \\ u_2 &= J(M_{nlin} - K_\omega\tilde{\omega} + \dot{\omega}_c - \omega_{bs}), \end{aligned}$$

where $s = \pm 1$ and ψ_{bs}, u_{bs}, w_{bs},and ω_{bs} are defined in eqns. 9, 8, 11, and 14, respectively. Because in this article, the θ and ϕ commands are externally generated, while ψ is used as a control variable, only yaw backstepping term, ψ_{bs}, must be defined for implementation of ω_c^o signal, which is done in Section IV. The terms θ_{bs} and ϕ_{bs} are identically zero. The term v_{bbs} is the vector notation of u_{bs} and w_{bs} terms while ω_{bs} is the vector notation of p_{bs}, q_{bs}, r_{bs} terms. For $s = 1$ the vehicle drives forward while for $s = -1$ the vehicle drives backward. Also, because this is trajectory following, it is assumed that the speed $\|(\dot{x}_c, \dot{y}_c)\|$ is non-zero and we have selected a solution for which the AUV forward velocity is always positive.

Eqn. (6), in Section IV, has the form,

$$\begin{bmatrix} u_c^o\ \mathrm{c}\psi_c^o \\ u_c^o\ \mathrm{s}\psi_c^o \end{bmatrix} = v_d - K_{xy}E$$

where

$$v_d = \begin{bmatrix} \frac{1}{\cos(\theta)}(-F_x + \dot{x}_c) \\ \frac{1}{\cos(\theta)}(-F_y + \dot{y}_c) \end{bmatrix} \text{ and } E = \begin{bmatrix} \frac{1}{\cos(\theta)}(\tilde{x}) \\ \frac{1}{\cos(\theta)}(\tilde{y}) \end{bmatrix}$$

The quantity v_d is the velocity vector that would cause the vehicle to follow the trajectory given that the vehicle was currently on the trajectory. The quantity $K_{xy}E$ is the feedback term that would cause the vehicle to converge toward the trajectory.

For the stability analysis to follow, the value of K_{xy} must be positive; however, its magnitude must be selected with care. The reasoning on how to select it is explained in detail in [1].

IV. OUTER LOOP: WAYPOINT GUIDANCE

The inputs to this outer loop are (after command filtering) $x_c(t)$, $y_c(t)$, $d_c(t)$, $\phi_c(t)$, $\theta_c(t)$, and the derivatives of these signals. This section is concerned with the control of $[x, y, d]$ by specification of desired values for $[u, \psi, w]$ which will be passed to the inner and middle loop controllers as command signals.

This section has two subsections. Subsection IV-A is concerned with control of $[x, y]$ by specification of $[u_c^o, \psi_c^o]$. Subsection IV-B is concerned with control of $[z]$ by specification of $[w_c^o]$.

A. Mode: XY Translation

Kinematic Analysis. Since v is not controllable and w is used to control depth we will control x and y by calculating appropriate u_d and ψ_d signals. For clarity, we rewrite x and y dynamics as

$$\begin{bmatrix} \dot{x} \\ \dot{y} \end{bmatrix} = \begin{bmatrix} u_x \\ u_y \end{bmatrix} \mathrm{c}\theta + \begin{bmatrix} F_x \\ F_y \end{bmatrix}$$

where

$$F_x = [\mathrm{c}\psi\mathrm{s}\theta\mathrm{s}\phi - \mathrm{c}\phi\mathrm{s}\psi]v + [\mathrm{c}\phi\mathrm{c}\psi\mathrm{s}\theta + \mathrm{s}\phi\mathrm{s}\psi]w,$$

$$F_y = [\mathrm{c}\phi\mathrm{c}\psi + \mathrm{s}\theta\mathrm{s}\phi\mathrm{s}\psi]v + [-\mathrm{c}\psi\mathrm{s}\phi + \mathrm{c}\phi\mathrm{s}\theta\mathrm{s}\psi]w,$$

and

$$\left.\begin{array}{l} u_x = u\ \mathrm{c}\psi \\ u_y = u\ \mathrm{s}\psi. \end{array}\right\} \tag{5}$$

The dynamic equation for x and y can be manipulated as follows

$$\begin{bmatrix} \dot{x} \\ \dot{y} \end{bmatrix} = \begin{bmatrix} F_x \\ F_y \end{bmatrix} + \begin{bmatrix} u_{x_c}^o \\ u_{y_c}^o \end{bmatrix} \mathrm{c}\theta + \begin{bmatrix} \tilde{u}_x \\ \tilde{u}_y \end{bmatrix} \mathrm{c}\theta$$

where $\tilde{u}_x = u_x - u_{x_c}$ and $\tilde{u}_y = u_y - u_{y_c}$. Again, there is another term, $[u_{x_c} - u_{x_c}^o, u_{y_c} - u_{y_c}^o]^\top$, that should be accounted for in the analysis, where $u_{x_c} = u_c \mathrm{c}\psi_c$, $u_{x_c}^o = u_{c_o}\mathrm{c}\psi_c^o$, etc. This term can be made arbitrarily small by increasing the bandwidth of the command filter that is used to compute u_c and ψ_c (and their derivatives) from u_c^o and ψ_c^o. The effect of this term is rigorously analyzed in [8]. Due to lack of space, the arguments are not repeated herein. We select signals $[u_{x_c}^o, u_{y_c}^o]^\top$ as

$$\begin{bmatrix} u_{x_c}^o \\ u_{y_c}^o \end{bmatrix} = \begin{bmatrix} \frac{1}{\cos(\theta)}(-F_x - K_{xy}\tilde{x} + \dot{x}_c) \\ \frac{1}{\cos(\theta)}(-F_y - K_{xy}\tilde{y} + \dot{y}_c) \end{bmatrix} \tag{6}$$

where K_{xy} is time varying and positive. The selection of the control signal above yields the x and y position error dynamic equations:

$$\begin{bmatrix} \dot{\tilde{x}} \\ \dot{\tilde{y}} \end{bmatrix} = \begin{bmatrix} -K_{xy}\tilde{x} \\ -K_{xy}\tilde{y} \end{bmatrix} + \begin{bmatrix} \tilde{u}_x \\ \tilde{u}_y \end{bmatrix} \mathrm{c}\theta \tag{7}$$

Two questions remain: how should we manipulate the $\tilde{u}_x$ and $\tilde{u}_y$ terms to allow a rigorous stability analysis that accounts for them; and, how should u_c^o and ψ_c^o be specified to achieve $[u_{x_c}^o, u_{y_c}^o]$? These issues are addressed in the following subsections.

Simplification of $\tilde{u}_x$ and $\tilde{u}_y$. These terms can be manipulated by two very similar approaches (derived in [1]). In either case the $\begin{bmatrix} \tilde{u}_x \\ \tilde{u}_y \end{bmatrix}$ term can be expressed in the following form

$$\begin{bmatrix} \tilde{u}_x \\ \tilde{u}_y \end{bmatrix} = A\tilde{u} + Bg(\tilde{\psi})\tilde{\psi}.$$

Thus, the position error dynamics can be expressed as

$$\begin{bmatrix} \dot{\tilde{x}} \\ \dot{\tilde{y}} \end{bmatrix} = \begin{bmatrix} -K_{xy}\tilde{x} \\ -K_{xy}\tilde{y} \end{bmatrix} + (A\tilde{u} + Bg(\tilde{\psi})\tilde{\psi})\cos(\theta)$$

which is a form suitable for stability analysis. The first term will be accommodated by the u backstepping control. The second term will be accommodated by the ψ backstepping control. Selecting Approach 1 in [1], we define u_{bs} and ψ_{bs} backstepping terms as

$$u_{bs} = \mathrm{c}\theta(\mathrm{c}\psi_c\tilde{x} + \mathrm{s}\psi_c\tilde{y}) \tag{8}$$

and

$$\begin{aligned} \psi_{bs} \quad = \quad & \mathrm{c}\theta \left\{ \left[u\ \mathrm{c}\psi_c \frac{\cos(\tilde{\psi}) - 1}{\tilde{\psi}} - u\ \mathrm{s}\psi_c \frac{\sin(\tilde{\psi})}{\tilde{\psi}} \right] \tilde{x} \right. \\ & \left. + \left[u\ \mathrm{s}\psi_c \frac{\cos(\tilde{\psi}) - 1}{\tilde{\psi}} + u\ \mathrm{c}\psi_c \frac{\sin(\tilde{\psi})}{\tilde{\psi}} \right] \tilde{y} \right\}. \end{aligned} \tag{9}$$

B. Mode: D Translation

The objective of this component of the outer loop is to select $w_c^o(t)$ to force $d(t)$ to converge to $d_c(t)$, where $d_c(t)$ and $\dot{d}_c(t)$ are known command signals.

Using the last row of the R matrix, the dynamics of d are

$$\dot{d} = -u\sin(\theta) + \cos(\theta)\sin(\phi)v + \cos(\theta)\cos(\phi)w.$$

Since desired values for u, ϕ, and θ are already specified and v is not controllable, assuming that $\theta \neq 90^\circ$ and $\phi \neq 90^\circ$, we will select the commanded value of

$$w_c^o = \frac{u\sin(\theta) - \cos(\theta)\sin(\phi)v - K_d\tilde{d} + \dot{d}_c}{\cos(\theta)\cos(\phi)}$$

for w to control d. This yields the closed loop depth error dynamic equation

$$\dot{\tilde{d}} = -K_d\tilde{d} + \mathrm{c}\theta\mathrm{c}\phi\tilde{w} + \mathrm{c}\theta\mathrm{c}\phi(w_c - w_c^o) \tag{10}$$

where the last term is dropped in the subsequent analysis due to space limitations, but can be analyzed rigorously by methods similar to those in [8].

Selecting the Lyapunov function (as in [1]) we can define the backstepping term

$$w_{bs} = \mathrm{c}\theta\mathrm{c}\phi\tilde{d} \tag{11}$$

that will be incorporated into the w inner loop control signal to cancel the sign indefinite portion in the stability analysis.

V. MIDDLE LOOP - ATTITUDE CONTROL

This control loop will be used by each of the outer loops and therefore it is described separately. The inputs to this outer loop are roll, pitch, and yaw commands, $\Theta_c = [\phi_c(t), \theta_c(t), \psi_c(t)]$ and the derivatives of these signals, which are produced by command filtering. Additional inputs are the roll, pitch, and yaw backstepping terms, Θ_{bs}.

For attitude control, based on eqn. (2), we define the signal

$$\omega_c^o = \Omega^{-1}\left(-K_\Theta\tilde{\Theta} + \dot{\Theta}_c - \Theta_{bs}\right)$$

where K_Θ is a positive definite matrix and $\tilde{\Theta}(t) = \Theta(t) - \Theta_c(t)$. Using this definition, the closed-loop tracking error corresponding to eqn. (2) is

$$\begin{aligned} \dot{\Theta} &= \Omega\omega_c^o + \Omega(\omega - \omega_c) + \Omega(\omega_c - \omega_c^o) \qquad (12)\\ &= -K_\Theta\tilde{\Theta} + \dot{\Theta}_c + \Omega\tilde{\omega} - \Theta_{bs} \\ \dot{\tilde{\Theta}} &= -K_\Theta\tilde{\Theta} + \Omega\tilde{\omega} - \Theta_{bs} \qquad (13) \end{aligned}$$

where the term $\Omega(\omega_c - \omega_c^o)$ is dropped after eqn. (12). This term can be made arbitrarily small by increasing the bandwidth of the command filter that is used to compute ω_c and $\dot{\omega}_c$ from ω_c^o. The effect of this term is rigorously analyzed in [8]. Due to lack of space, the arguments are not repeated herein. To compensate for the sign indefinite $\tilde{\omega}$ term in the stability analysis the term ω_{bs} in Section VI is defined as

$$\omega_{bs} = \Omega^\top\tilde{\Theta}. \tag{14}$$

VI. INNER LOOP

The inputs to the inner loop are u_c, $\dot{u}_c$, w_c, $\dot{w}_c$, ω_c, $\dot{\omega}_c$, u_{bs}, w_{bs},and ω_{bs}. Each of these input signals is defined by one of the middle or outer loops as will be described in the sequel. Each of the signals u_c, w_c, and ω_c are commands to the inner loop. The signals $\dot{u}_c$, $\dot{w}_c$, and $\dot{\omega}_c$ are the derivatives of the commands. The signals are u_{bs}, w_{bs} and ω_{bs} are backstepping terms defined to cancel sign-indefinite terms in the stability analysis.

The inner loop control signals are

$$\begin{aligned} u_1 &= M(F_{nlin} - K_v\tilde{v}_b + \dot{v}_{bc} - v_{bbs}) \qquad (15)\\ u_2 &= J(M_{nlin} - K_\omega\tilde{\omega} + \dot{\omega}_c - \omega_{bs}) \qquad (16) \end{aligned}$$

with the thrust vector defined as

$$T = \begin{bmatrix} L_f \\ L_m \end{bmatrix}^{-1} \begin{bmatrix} u_1 \\ u_2 \end{bmatrix}$$

where $\tilde{v}_b = v_b - v_{bc}$, $\tilde{\omega} = \omega - \omega_c$, and K_v and K_ω are positive definite matrices.

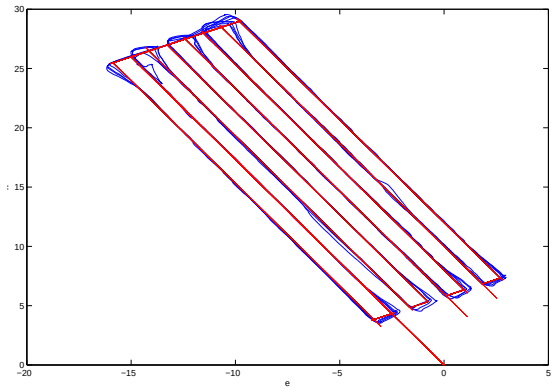

Fig. 1. 2 D Position vs. Time: Blue line is the actual vehicle trajectory, black line is the command, and the red line is filtered command

With this choice of the control signal and the fact that $\dot{\tilde{v}}_b = \dot{v}_b - \dot{v}_{bc}$ and $\dot{\tilde{\omega}} = \dot{\omega} - \dot{\omega}_c$, the dynamics of the tracking errors are

$$\begin{aligned} \dot{\tilde{u}} &= -K_u\tilde{u} - u_{bs} \\ \dot{\tilde{w}} &= -K_w\tilde{w} - w_{bs} \\ \dot{\tilde{\omega}} &= -K_\omega\tilde{\omega} - \omega_{bs} \end{aligned}$$

VII. AUVFEST RESULTS

During AUVFest, we accomplished 12 hours of in-water demonstration time. The goal was to accurately navigate in the harsh environment under the hull of a ship while maintaining the distance from the ship for optimal imaging sonar positioning. All hull search vehicle behaviors were demonstrated with the following unique capabilities: autonomous mission execution with intervention capability, hull search conducted using side look sonar, sensors parameters optimized by operator during mission, real-time topside display of Sound Metrics DIDSON High Definition Imaging Sonar and Marine Sonics 1800kHz Side Looking Sonar, vehicle position and status information embedded in DIDSON sensor data and Joint Architecture for Unmanned Systems (JAUS) communication protocol implemented on UUV. The 2D position plot is shown Figure 1. Great trajectory tracking performance can be noticed since the vehicle maintained its track-line even with the presence of side currents. This is greatly desired capability for this type of mission since 100 percent ship-hull coverage is required. The position plot showing north, east, down, and altitude position versus time is shown in Figure 2, while the attitude (roll, pitch, yaw) plot is shown in Figure 3. Vehicle's horizontal and vertical velocities are shown Figure 4, while the angular rates (roll, pitch, yaw rate) plot is shown in Figure 5. Excellent tracking performance can be observed, for instance, maximum depth variations were around 5 cm, maximum roll variations were around 4 degrees, while maximum variations in pitch were around 2 degrees.

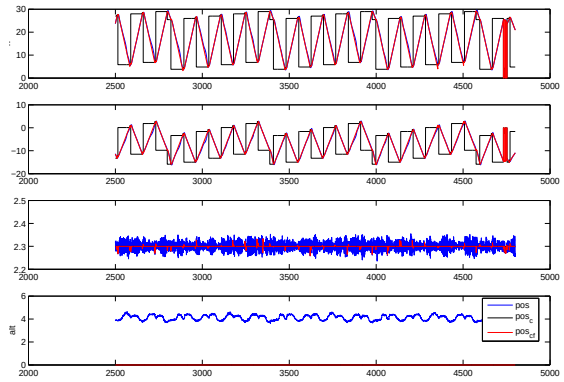

Fig. 2. North, East, and Down Position vs. Time: Blue line is the actual vehicle trajectory, black line is the command, and the red line is filtered command

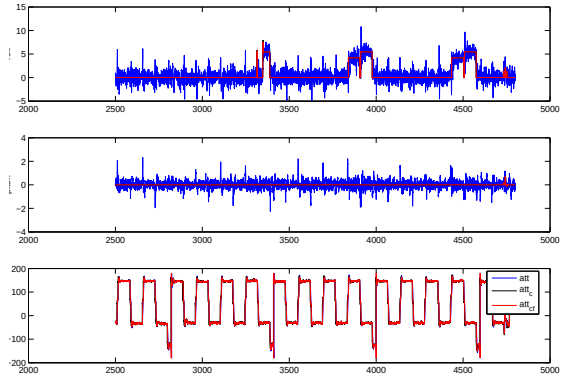

Fig. 3. Attitude vs. Time: Blue line is the actual vehicle attitude, black line is the command, and the red line is filtered command

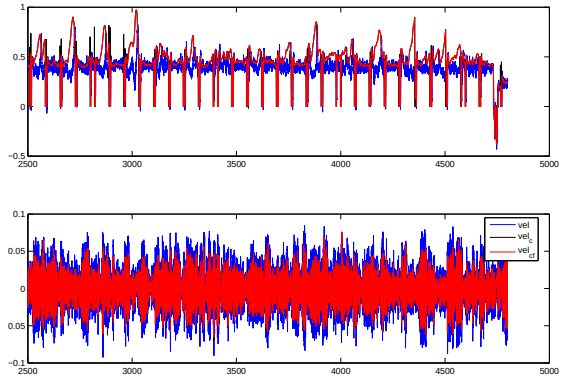

Fig. 4. Velocities vs. Time: Blue line is the actual vehicle velocity, black line is the command, and the red line is filtered command

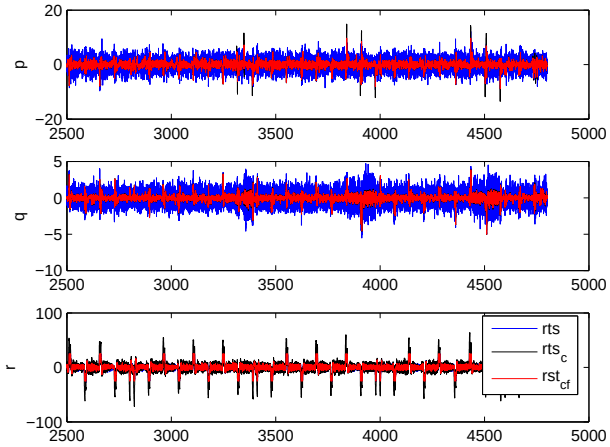

Fig. 5. Angular Rates vs. Time: Blue line is the actual vehicle angular rate, black line is the command, and the red line is filtered command

VIII. CONCLUSION AND FUTURE WORK

This article has discussed the design and derivation of a command filtered, vector backstepping approach to design a stable translational and attitude controller (i.e., $y = [x(t), y(t), d(t), \psi(t), \theta(t)]^\top$) applicable to an underactuated AUV. The mission scenario specifies the position and attitude commands which are command filtered to produce inputs (together with their derivatives) for the outer loop and middle loop controllers. The commands, such as horizontal and vertical velocities (u_c,w_c) and angular rates (p_c,q_c,r_c) are generated by the outer and middle loop, command filtered, and are inputs (together with their derivatives) to the velocity and angular rate inner loop controllers. The inner loop determines the appropriates thrust forces. The article has presented both the control law derivation and the actual in-water results. The plan is to design additional outer loop controllers to increase the vehicle maneuverability and capability. The outer loop controllers are defined for different vectors of outer loop control variables as specified by the vector of outputs y. Other example behaviors expected to be implemented in the future include translation with unspecified attitude $y = [x(t), y(t), d(t), u(t)]^\top$ and station keeping $y = [x, y, d, \psi]^\top$.

IX. ACKNOWLEDGMENTS

The authors gratefully acknowledge the ONR and SSC-SD's ILIR program for funding V. Djapic'c PhD work and

the work described in this paper. In addition, the authors gratefully thank PMS EOD and EODTECHDIV sponsors whose support enabled the implementation of the algorithms onboard of AUV and proved the concept of the research approach.

REFERENCES

[1] V. Djapic, J. A. Farrell J. A., P. Miller, Back-stepping applied to Translational and Attitude Control of Underactuated Autonomous Underwater Vehicle (AUV), submitted to 46th IEEE Conference on Decision and Control, New Orleans, Louisiana USA, 2007.

[2] R. M. Arrieta, B. Granger, V. Djapic, "Highlight the Operational Value of the Adaptive Mission Planner with respect to Searching Ship Hulls," SSC-SD White Paper, 26 Jan 2004.

[3] R. M. Arrieta, J. A. Farrell, W. Li, S. Pang, Initial Development and Testing of an Adaptive Mission Planner for a Small Unmanned Underwater Vehicle, Proc. Of the 22nd Int. Conf. On Offshore Mechanics and Artic Engi-neering, OMEA2003-37273, AMSE.

[4] Fossen T., Marine Control Systems: Guidance, Navigation, and Control of Ships, Rigs and Underwater Vehicles, Marine Cybernetics, Trondheim, Norway, 2002.

[5] J. A. Farrell, W. Li, S. Pang, R. Arrieta, Chemical Plume Tracing Experimental Results with a REMUS AUV, MTS/IEEE Oceans 2003, pp. 962-968.

[6] J. A. Farrell, S. Pang, and W. Li, "Chemical Plume Tracing via an Autonomous Underwater Vehicle" IEEE J. of Oceanic Engineering, submitted Sept 29, 2003. resubmitted August 16, 2004. Accepted September 2004.

[7] J. A. Farrell, S. Pang, W. Li., and R. Arrieta "Biologically Inspired Chemical Plume Tracing Demonstrated on an Autonomous Underwater Vehicle", accepted for publication at IEEE Systems, Man, and Cybernetics Con-ference, September 2004, Hague, Netherlands.

[8] J. A. Farrell, M. Polycarpou, M. Sharma, W. Dong, "Command Filtered Backstepping," Submitted to IEEE Trans. on Automatic Control, March 2007.

[9] US Navy UUV Masterplan 2004, in press

[10] Krstic, M., I. Kanellakopoulos, P.V. Kokotovic, (1995) Nonlinear and adaptive Control design, N.Y., Wiley.